JOURNAL OF MATERIALS SCIENCE 32 (1997) 4397–4403

Investigation of debonding processes in particle-filled polymer materials by acoustic emission

Part I *Acoustic emission and debonding stress*

R. KRAUS, W. WILKE
Abteilung Experimentelle Physik, Universität Ulm, D-89069 Ulm, Germany
A. ZHUK
Division of Applied Science, Harvard University, Cambridge, USA
I. LUZINOV, S. MINKO, A. VORONOV
Department of Physical Chemistry Institute, Ukrainian Academy of Sciences, Lviv, Ukraine

Debonding processes in model composites under tensile deformation were investigated by acoustic emission analysis. The composites were prepared from epoxy and polyethylene matrix filled with glass beads of various sizes and with different coatings. The detected acoustic emission signals were identified as debonding processes at the filler–matrix interphase, and are discussed as a rupture process on the basis of the Weibull probability distribution function. For the model composites, the effect of the filler size is discussed using a theory based on Griffith's criterion of rupture.

1. Introduction

During deformation processes in particle-filled polymer composites, the most common failure mechanism is debonding at the filler–matrix interface. For a better insight into these processes, it is desirable to investigate these mechanisms using model systems, that allow a detailed analysis of the influence of filler and matrix properties. In the present work, we used acoustic emission analysis to investigate debonding processes during tensile loading in different polymer materials (epoxy, polyethylene) filled with glass beads of various sizes and surface treatment. Zhuk *et al.* [1] investigated debonding processes in epoxy composites filled with glass beads using optical microscopy to determine the debonding stress. The acoustic emission analysis technique offers the capability of monitoring the debonding processes at much higher numbers and rates to improve statistical analysis.

2. Theory

2.1. Griffith theory of debonding

Based on the Griffith [2] theory of rupture, Zhuk *et al.* developed a theory to describe debonding processes in particle-filled composite materials [1]. The change in free energy, ΔF, is used as the criterion for the debonding of the polymer matrix from the filler surface. This is given by the difference between the surface energy, F_s, needed for the detachment of the matrix from the filler and the released elastic energy, F_e. Debonding is only possible for $\Delta F < 0$.

$$\Delta F = F_s - F_e < 0 \tag{1}$$

The influence of filler properties (surface structure, particle size) on debonding processes, e.g. the debonding stress, can be discussed using this theory. A detailed description is given elsewhere [1, 3, 4].

The filler surface is never perfectly smooth. Defects on the surface of the filler particles act as nuclei for later debonding under tensile stress. The relationship between the filler size and the structure of the filler surface, i.e. the defect size, determines the scaling of the stress of debonding.

(i) if the size, d, of the defects is independent of filler radius, R, for sufficiently small defects ($d < R/3$) the influence of filler size on the debonding stress, σ_d, becomes negligible

$$\sigma_d \propto \text{constant} \tag{2}$$

(ii) If the size of the defects is proportional to the filler size, the above-mentioned theory yields the relation

$$\sigma_d \propto R^{-1/2} \tag{3}$$

This behaviour was observed by Gent [4] in elastomers filled with glass beads.

2.2. Weibull distribution function

The debonding of the matrix from the filler surface resembles some kind of rupture process. For the

0022–2461

statistical description of strength and rupture data the Weibull distribution function is very common [5].

If the conditions of the deformation process meet the following requirements, the Weibull distribution should also be applicable to the description of the debonding of filler particles in a polymer matrix.

(i) The filler particles must be homogeneously distributed in the matrix.

(ii) The stress field in the vicinity of all filler particles must be identical and definite for a given state of deformation.

(iii) The filler particles may not interfere with each other in their stress fields.

Then the probability for failure at a stress $\sigma' < \sigma$ is given by

$$P(\sigma) = 1 - \exp\left[-\left(\frac{\sigma}{\sigma_1}\right)^m \right] \quad (4)$$

A lower bound for the strength, σ_0, can be taken into account by

$$P(\sigma) = 1 - \exp\left[-\left(\frac{\sigma - \sigma_0}{\sigma_1 - \sigma_0}\right)^m \right] \quad (5)$$

The distributive form $p(\sigma)$ of the function is also very common for easier interpretation

$$p(\sigma) = \frac{dP}{d\sigma} \quad (6)$$

$$= \frac{m}{\sigma_1 - \sigma_0}\left(\frac{\sigma - \sigma_0}{\sigma_1 - \sigma_0}\right)^{m-1} \exp\left[-\left(\frac{\sigma - \sigma_0}{\sigma_1 - \sigma_0}\right)^m \right] \quad (7)$$

where σ_0 is the lower bound for failure, σ_1 the stress parameter, and m the Weibull exponent.

3. Experimental procedure

3.1. Materials and specimens

Two different types of model composite were prepared. One series of composites was made from epoxy resin matrix filled with glass beads of various sizes and surface coatings, to investigate the influence of filler properties on the failure process. Another series was made from different types of polyethylene matrix filled with uncoated glass beads of various sizes, to investigate the influence of the matrix properties. All composites were prepared as plates, from which dog-bone shaped specimens were cut.

3.1.1. Epoxy composites

The specimens were prepared by mixing of epoxy resin (diglycidylresorcinolether, $C_{12}H_{14}O_4$), initiator (*m*-phenylene diamine, $C_6H_8N_2$) and filler, and polymerized under rotation at $T = 64\,^{\circ}C$ to avoid precipitation of the filler particles and with further curing by a two-step temperature procedure ($T = 64\,^{\circ}C$, 4 h; $T = 130\,^{\circ}C$, 8 h). The filler consists of glass beads of various sizes (50–63, 80–90, 100–125, 160–200, 315–400 μm) the filler content was a volume fraction of 1% for all sizes. The surface of the glass beads was treated by polymers in two steps. In the first stage, the surface was covered by copolymer of 5-tert-butyl-peroxy-5-methyl-1-hexen-3-yne with maleic anhydride (1:1 mol ratio), $M_n = 3000$ by adsorption of the copolymer from solution (further denoted as peroxide copolymer). The adsorption amount of the copolymer was $8\,mg\,m^{-2}$.

This first layer of peroxide copolymer has the function of an initiator of graft radical polymerization of styrene and butylacrylate, due to the process of polymerization on the surface of the beads dispersed in monomer solution at $T = 120\,^{\circ}C$. The amount of grafted polymers was about $30\,mg\,m^{-2}$, which corresponds to a thickness of the polymer layer of 0.1–0.2 μm (obtained by electron microscopy) [6–8].

3.1.2. Polyethylene composites

Three different types of linear polyethylene of medium density were used as matrix materials for a series of composites filled with glass beads of various sizes.

The polyethylene material is a copolymer of ethylene and 1-hexene and was produced by Tiszai Vegiy, Hungary, and distributed under the trade mark TIPELIN. The names BS-501-17, FA-470-02 and FB-472-20 denote different ethylene–hexene–copolymers with different degrees of branching and density. Some physical data on the different types are given in Table 1.

The polyethylene matrix was filled with glass beads produced and distributed by Dragon-Werk, Bayreuth, Germany under the trade-mark DRAGONIT 25. Three fractions of different size were used: 80–110, 160–250 and 290–420 μm.

The composites were produced by milling the polyethylene granulate to 0.3 mm average grain size after cooling in liquid nitrogen, powder mixing with the filler beads, and melting under pressure ($p = 20$ bar) at a temperature of $T = 200\,^{\circ}C$. Then the composites were cooled slowly ($\sim 2\,K\,min^{-1}$) to room temperature.

3.2. Test methods

Tensile tests were performed on a Zwick 1445 testing machine at a constant speed of $d\lambda/dt = 1.25 \times 10^{-3} s^{-1} (\lambda = l/l_0)$. Acoustic emission was monitored on an AET Model 5500 system. The AET 5500 was set

TABLE I Physical data of TIPELIN polyethylenes

Tipelin type	$\bar{M}_w$	$\bar{M}_n$	ε	ρ(g cm^{-3})	X_c	T_m(°C)
BS-501-17	198000	12000	0.6	0.950	0.75	122
FA-470-02	187000	20000	2.0	0.947	0.73	119
FB-472-20			2.0	0.950	0.73	119

$\bar{M}_w$ = molecular weight, weight average; $\bar{M}_n$ = molecular weight, number average; ε = degree of branching = CH_3-end groups/1000 CH_2-units; ρ = density; X_c = degree of crystallinity from WAXS or DSC; T_m = melting temperature

up in single sensor mode with one transducer attached to the specimen by a spring clamp. The transducer was a standard AET AC175L with a resonant frequency of 175 kHz and a sensitivity better than -72 dB referred to 1 V μbar^{-1}. The detected signals were passed through a band-pass filter FL-12 with a flat frequency response between 125 and 250 kHz. Then they were preamplified in an AET Model 140/160 B preamplifier with a total gain of 40/60 dB and a flat frequency response between 1 kHz and 2 MHz. Final amplification was performed by the AET Signal Processing Unit with 30 dB. To eliminate noise events only acoustic emission events with three or more ring down counts (number of threshold crossings by the signal voltage) were accepted [9].

The force and deformation data were input into the AET 5500 through the analogue input channels. As the greater part of the specimen is covered with clamp and sensor, optical strain measurement cannot be used here. The deformation of the samples is practically homogeneous. Therefore, the strain, λ, is determined from the traverse distance, Δl, by $\lambda = (\Delta l + l_0)\ /l_0$. For each acoustic emission event strain, λ, stress, σ, peak amplitude, $A = 20\log_{10}(U/U_{\mathrm{ref}})$ dB (where U is the signal voltage, and U_{ref} the reference voltage), event duration and number of ring down counts (i.e. threshold crossings) were recorded.

The data were processed and analysed off-line by custom-made software in order to avoid a reduction of system performance by real-time analysis. In a first step, a device-independent file containing the values of the variables strain, λ, stress, σ, and peak amplitude, A, was calculated from the raw AET 5500 data. These files were used to calculate frequency diagrams with respect to strain, λ, and stress, σ, for further analysis using *MATLAB for Windows* and MicroCal ORIGIN.

4. Results

Experiments performed by Faudree *et al.* [10] and Shirouzu *et al.* [11] showed that the number of acoustic emission events correlates directly with the number of debonding acts. Experiments with specimens of unfilled matrix show no noticeable acoustic emission. At low stress there is practically no acoustic emission. With increasing stress, the number of acoustic emission events per stress interval increases rapidly and reaches its maximum. Then it decreases again (Fig. 1). This maximum is interpreted as the average debonding stress. For a quantitative evaluation there are two possibilities.

(i) The acoustic emission is determined with reference to strain $\lambda = l/l_0$ by counting the number of events in each strain interval, $\Delta\lambda$, in the following denoted as $\mathrm{d}N/\mathrm{d}\lambda$. Then the modal value of the debonding stress, σ_{d}, is given by the stress $\sigma(\lambda_{\mathrm{d}})$, corresponding to the strain λ_{d}, where the number of acoustic emission events per stress interval $\mathrm{d}N/\mathrm{d}\lambda$ reaches its maximum. This approach does not require any special assumptions about the deformation process.

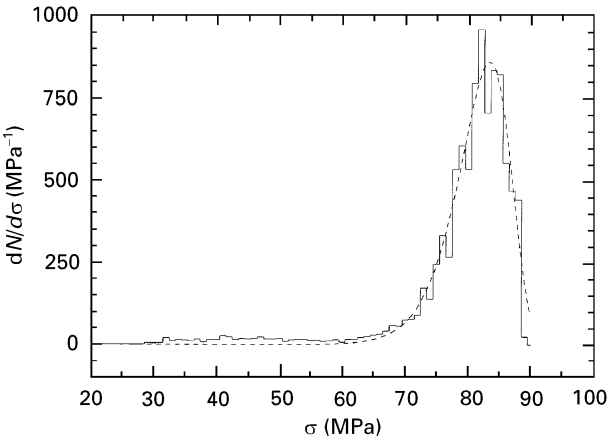

Figure 1 Number of acoustic emission events per stress interval for epoxy composite filled with 100–125 μm glass beads coated with peroxide copolymer. $\sigma_d = 83 \pm 1$ MPa.

(ii) If the conditions of the process of deformation and debonding meet the above stated requirements (Section 2.2), it is possible to discuss the debonding as a rupture process using the Weibull distribution for the acoustic emission with reference to stress. $\mathrm{d}N/\mathrm{d}\sigma$ is given by the number of events within each stress interval, $\Delta\sigma$. Therefore, the curve of the acoustic emission counts per stress interval, $\mathrm{d}N/\mathrm{d}\sigma(\sigma)$, is numerically fitted (least square fit using a Levenberg–Marquardt algorithm) by a Weibull distribution function of the form

$$\phi(\sigma) = N_0 \frac{m}{\sigma_1 - \sigma_0}\left(\frac{\sigma - \sigma_0}{\sigma_1 - \sigma_0}\right)^{m-1} \times \exp\left[-\left(\frac{\sigma - \sigma_0}{\sigma_1 - \sigma_0}\right)^{m}\right] \tag{8}$$

where N_0 is the normalization parameter, σ_0 the lower bound for failure, σ_1 the stress parameter, and m the Weibull exponent.

To characterize the debonding stress we use the modal value, σ_{d}, which is determined by the maximum of the fitted distribution function

$$\sigma_{\mathrm{d}} = \sigma_0 + (\sigma_1 - \sigma_0)\left(\frac{m-1}{m}\right)^{1/m} \tag{9}$$

Fig. 1 shows an example for this type of analysis with a stress interval $\Delta\sigma = 1$ MPa for the frequency curve. The discontinuous style of the curve is caused by statistical variation. The given errors for the modal values of the debonding stress were derived from the standard deviations (square root of Weibull variances) of the fitted parameters.

4.1. Epoxy composites

Specimens of epoxy composites filled with glass beads with different polymer coatings and of various sizes have been investigated by tensile loading until rupture at room temperature ($T = 22\,^{\circ}$C). The modal value of the debonding stress was obtained by fitting a Weibull distribution function to the number of acoustic emission events per stress interval, $\mathrm{d}N/\mathrm{d}\sigma$.

The samples filled with glass beads, which were treated only with the peroxide copolymer, show comparatively high values for the average debonding stress. This indicates good adhesion between matrix and filler surface. Additional coatings prepared from polybutylacrylate (PBA) or polystyrene (PS) decrease the debonding stress. For the samples with polystyrene, the debonding stress is minimum. Here a second maximum of the number of acoustic emission events per stress interval, $dN/d\sigma$, occurs at higher stress. The reason for this could be clarified by investigations of the deformation process by optical microscopy. It was found that the first maximum of $dN/d\sigma$ correlates with the debonding of the spherical filler particles on one polar side, that leads to a local decrease of the stress concentration near the filler particle. When the external stress is increased further, the stress concentration in the vicinity of the filler particle increases again and the spherical filler particles become debonded at the other pole too. This second stage of debonding leads to a second maximum of $dN/d\sigma$ and can only be observed when the debonding stress is low compared to the failure stress of the matrix. Otherwise the sample will break before this second stage of debonding occurs.

The results for the modal values of the debonding stress for the samples with different filler sizes and coatings are given in Table II. The modal values, σ_d, were determined by fitting a Weibull distribution function as described above. The given errors were derived from the standard deviations (square roots of Weibull variances) of the fitted parameters.

The properties of the interphase between the polymer matrix and the filler particles strongly determine the process of debonding. Therefore, for all samples, the fracture surface has been investigated by scanning electron microscopy. The peroxide copolymer does not form a dense layer and therefore the epoxy matrix has part contact with the filler surface (Fig. 2). This yields a comparatively high debonding stress close to the strength of the polymer matrix. The glass beads with polybutylacrylate coating exhibit a porous surface structure, that may also permit some contact between epoxy matrix and glass surface (Fig. 3). The filler particles covered with polystyrene show a smooth surface, that is detached from the surrounding matrix (Fig. 4).

TABLE II Modal value of debonding stress: epoxy-composites

Coating	Filler size, $2R$(μm)	Modal value of debonding stress, σ_d(MPa)
Peroxide-copolymer	50–63	81 ± 2
	100–125	83 ± 2
	160–200	77 ± 3
	315–400	59 ± 3
Polybutylacrylate (additional)	50–63	61 ± 2
	80–90	72 ± 3
	100–125	45 ± 2
	160–200	75 ± 2
Polystyrene (additional)	50–63	43 ± 1
	100–125	43 ± 2
	160–200	42 ± 2
	315–400	33 ± 2

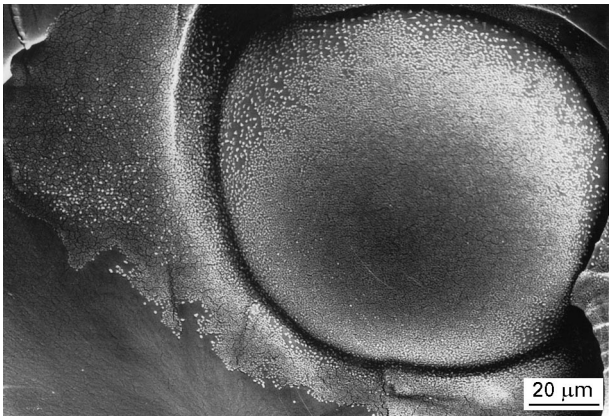

Figure 2 Scanning electron micrograph of the fracture surface of epoxy composite filled with glass beads coated with peroxide copolymer only.

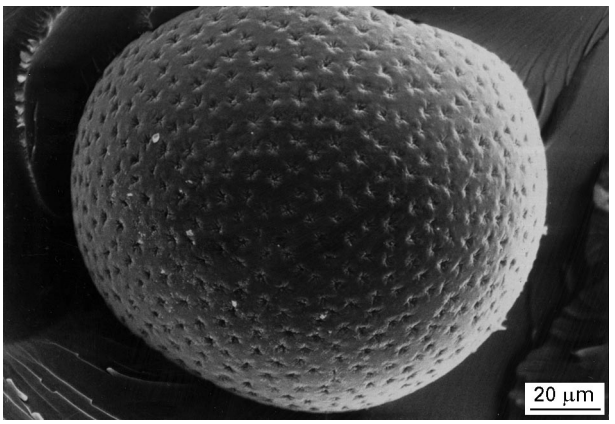

Figure 3 Scanning electron micrograph of the fracture surface of epoxy composite filled with glass beads coated with an additional layer of polybutylacrylate.

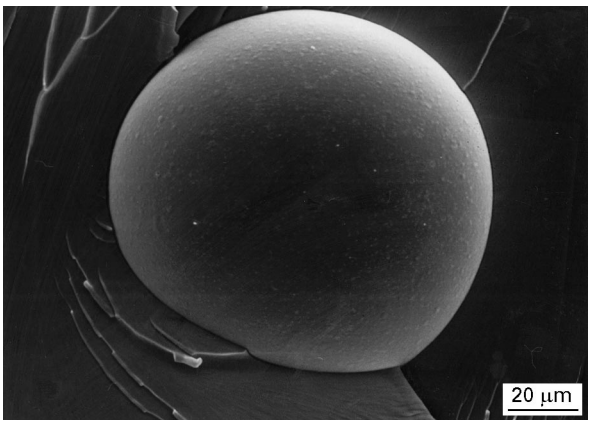

Figure 4 Scanning electron micrograph of the fracture surface of epoxy composite filled with glass beads coated with an additional layer of polystyrene.

4.2. Polyethylene composites

Specimens of polyethylene composites filled with glass beads of various size have been investigated by tensile loading at room temperature ($T = 22\,^{\circ}C$). The

comparatively good adhesion between the matrix BS-501-17 (low degree of branching) leads to the highest debonding stress for all filler sizes. Here the number of detected acoustic emission events is smaller than for the other specimens. In this case the debonding process is not completed within the range of elastic deformation, but extends to viscoelastic and plastic deformation. Therefore, the deformation process does not comply with the preconditions of the Weibull analysis. They require that the stress field in the vicinity of all filler particles must be identical and definite for a given deformation state. Plastic deformation leads to a variety of debonding acts, which occur at the same stress level, but at different deformation states. So the debonding stress can only be analysed through the number of acoustic emission events with reference to strain $dN/d\lambda$ (Fig. 5). The modal value of the debonding stress, σ_d, is given by the stress $\sigma(\lambda_d)$, corresponding to the strain λ_d, where the number of acoustic emission events per stress interval, $dN/d\lambda$, reaches its maximum. The results of this analysis are given in Table III. The errors for BS-501-17 represent the variabilities of different tests.

The modal values of the debonding stress for the composites prepared from matrices FA-470-02 and FB-472-20 (higher degree of branching) are much lower and differ only slightly. Here the debonding process is completed within the range of elastic deformation and it is possible to determine the modal value of the debonding stress from Weibull distribution analysis of $dN/d\sigma$ as described in Section 4.1. A comparison of the modal values for the debonding stress obtained from $dN/d\sigma$ and $dN/d\lambda$ shows good agreement within the range of error, that was derived from the standard deviation of the fitted Weibull parameters and is given in Table III. For all samples, the modal value of the debonding stress decreases with increasing filler size.

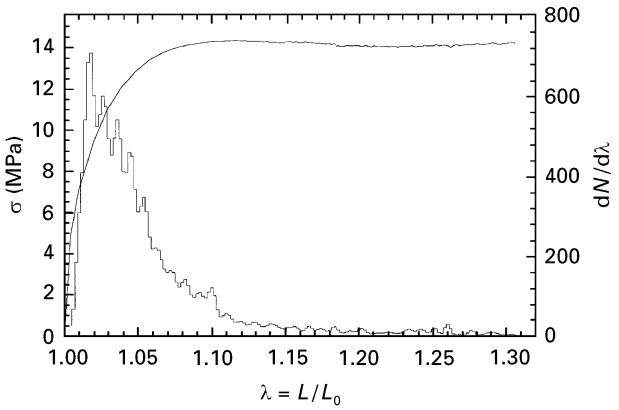

Figure 5 Number of acoustic emission events per strain interval and stress as function of strain for polyethylene (BS-501-17) composite filled with 80–110 μm glass beads. $\lambda_d = 1.020$, $\sigma(\lambda_d) = 9.6 \pm 1$ MPa.

TABLE III Modal value of debonding stress: polyethylene composites

Matrix	Filler size, $2R$(μm)	Modal value of debonding stress, σ_d(MPa)
BS-501-17	80–110	9.6 ± 1
	160–250	8.8 ± 1
	290–420	7.0 ± 1
FA-470-02	80–110	6.0 ± 1
	160–250	5.1 ± 1
	290–420	5.0 ± 1
FB-472-20	80–110	5.8 ± 1
	160–250	4.9 ± 1
	290–420	4.7 ± 1

5. Discussion

The influence of the filler size on the debonding stress can be shown by plotting the debonding stress versus the reciprocal square root of the filler particle radius, $R^{-1/2}$. For the following discussion we make the assumption that the debonding stress is proportional to its experimental modal value, σ_d. Therefore, Equations 2 and 3 should be valid also for the experimental values σ_d. The radius, R, is given by the mean value of the size distribution.

5.1. Epoxy composites

The scaling behaviour of the debonding stress for epoxy composites with different filler sizes is intermediate between the extreme cases described in Section 2.1. The composites with filler coated only by peroxide copolymer show, for large filler particles, a clear decrease of debonding stress. This is interpreted as a consequence of the increasing roughness of filler surface, that has close contact with the epoxy matrix. On the other hand, for the samples with additional polystyrene (PS) coating, the debonding stress is nearly constant (Fig. 6). Investigations by electron microscopy (SEM) show, that the grafted polystyrene forms a smooth layer on the filler surface. Therefore, the size of surface defects is determined by the structure of the PSA layer, that can be considered as independent from size. The debonding stress of

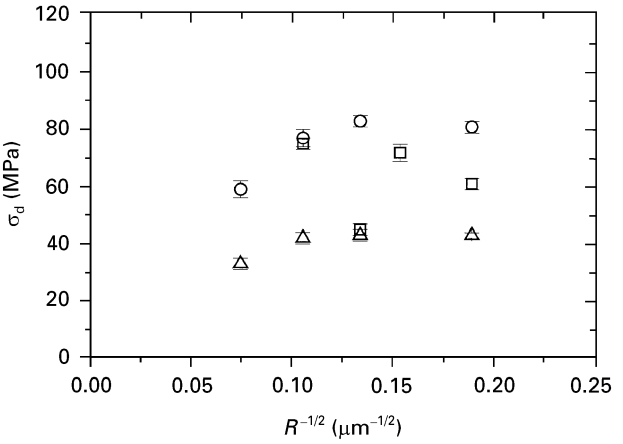

Figure 6 Dependence of the modal value of debonding stress on filler size for epoxy composites filled with glass beads with different coatings and sizes. (○) Peroxide copolymer only, (□) polybutylacrylate, (△) polystyrene.

polybutylacrylate (PBA) samples varies strongly for different filler sizes. The elastic modulus of PBA is comparatively low ($E_{PBA} \approx 0.1\, E_{epoxy}$), variations in thickness and porosity due to preparation of the polymer layer on the filler surface have a strong effect on the debonding process.

5.2. Polyethylene composites

The polyethylene composites also show small influence of the filler size on the debonding stress. As the filler particles were not treated with any coatings, the filler surface structure determines the stress of debonding. Obviously, the roughness of the glass beads grows only slightly with increasing particle size. The debonding stress is higher for the composites with a matrix with a low degree of branching (BS-501-17) and lower for those with a higher degree of branching (FA-470-02, FB-472-20) (Fig. 7).

Investigations of the superstructure of the matrix by electron microscopy (TEM) show a crystal lamellar structure [12], with increasing tendency to form clusters with decreasing degree of branching. Although the polymers FA-470-02 and FB-472-20 have the same degree of branching ($\varepsilon = 2.0\, CH_3/10^3C$), the latter exhibit fewer clusters. Possibly the higher degree of crystallinity of BS-501-17 and the formation of lamellar clusters leads to an improved adhesion of this matrix on the filler surface.

Experiments with small-angle scattering of synchrotron radiation (SAXS) at HASYLAB (DESY, Hamburg) during deformation of unfilled matrix samples show the formation of microcracks [12, 13]. The tendency of microcracking decreases with an increasing degree of branching (Fig. 8). Investigations by Payer [13] of fibre-filled polyethylene composites, show much stronger scattering already at small strain for samples with matrix BS-501-17 compared to the matrix types with a higher degree of branching (Fig. 9).

Acoustic emission measurements, however, pointed out that there is no measurable acoustic emission. Obviously, the amount of mechanical energy that is released by the formation of a microcrack, is too small to trigger the acoustic emission detector.

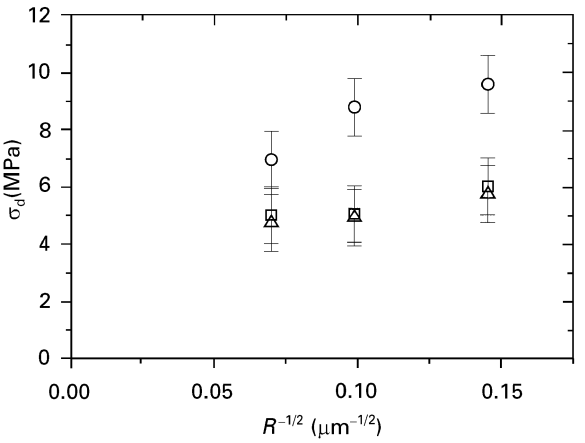

Figure 7 Dependence of modal value of debonding stress on filler size for polyethylene composites filled with glass beads with different sizes. (○) BS-501-17, (□) FA-470-02, (△) FB-472-20.

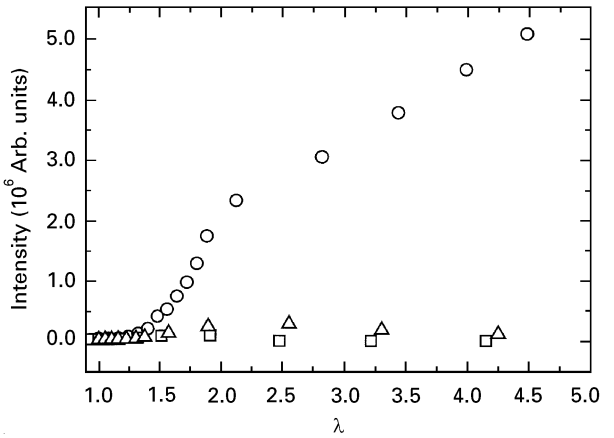

Figure 8 Intensity of small-angle X-ray scattering by micro-cracks as a function of strain for unfilled polyethylene matrix. (○) BS-501-17, (□) FA-470-02, (△) FB-472-20.

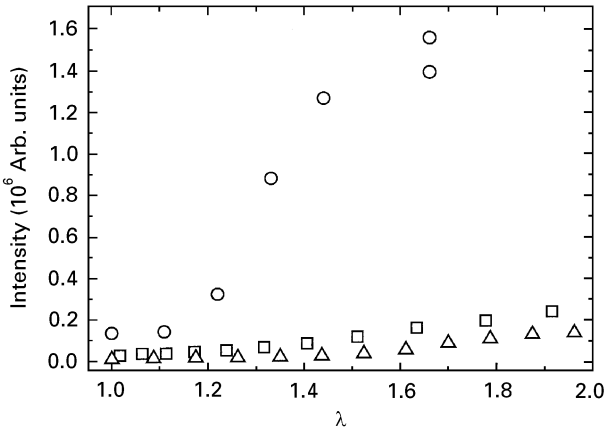

Figure 9 Intensity of small-angle X-ray scattering by micro-cracks as a function of strain for polyethylene composites filled with short glass fibres. (○) BS-501-17, (□) FA-470-02, (△) FB-472-20.

These results indicate that debonding processes, which cause acoustic emission, and the formation of microcracks, simultaneously act as parallel channels of energy dissipation. It is supposed that the composites with BS-501-17 matrix release deformation energy mainly by microcracking, while samples with a higher degree of branching dissipate energy by debonding processes, that are detected as acoustic emission events.

6. Conclusion

Debonding processes in model composites under tensile deformation were investigated by acoustic emission analysis. The composites were prepared from epoxy and polyethylene matrix filled with glass beads of various sizes and with different coatings. The detected acoustic emission signals, which were identified as debonding processes at the filler–matrix interphase, are discussed as a rupture process. The number of acoustic emission events per stress interval can be described by a Weibull distribution function, that allows a more precise determination of the modal

value of the debonding stress. The debonding stress depends on filler and matrix properties. Epoxy composites filled with glass beads show a strong influence of the polymer coating of the filler surface on the debonding stress. These results are compared to images of the fracture surface obtained by scanning electron microscopy. The influence of the matrix properties on the debonding process was investigated by model composites with a polyethylene matrix with different degrees of branching, filled with untreated glass beads of various sizes. For both model composites, the effect of the filler size has been discussed using a theory based on Griffith's criterion of rupture.

Acknowledgements

We are grateful for the support of the Deutsche Forschungsgemeinschaft (DFG). The collaboration between the groups from Ulm (Germany) and Lviv (Ukraine) was supported by the NATO Scientific Affairs Division under HTECH.LG.940579. The experiments with synchrotron radiation were funded by the German Federal Ministry for Research and Technology (BMFT), project number 055VUAXII.

References

1. A. V. ZHUK, V. G. KNUNYANTS, V. G. OSHMYAN and V. A. TOPOLKARAEV, *J. Mater. Sci.* **28** (1993) 4595.
2. A. A. GRIFFITH, *Trans. R. Soc. Lond.* **A221** (1920) 163.
3. A. N. GENT, *J. Mater. Sci.* **15** (1980) 2884.
4. A. N. GENT and BYOUNGKYEU PARK, *ibid.* **19** (1984) 1947.
5. W. WEIBULL, *J. Appl. Mech.* **18** (1951) 293.
6. S. S. MINKO, I. LUZINOV, A. VORONOV and R. MUSIY, *Ukrain. Chemich. Z.* **60** (1994) 727.
7. S. S. MINKO, I. LUZINOV, A. VORONOV and V. TOKAREV, "Polymer at Interphase, Synthesis, Adsorption, Conformation and Reactivity", a report. State University Lvivska Polytechnika (1994).
8. R. KRAUS, A. ZHUK, I. LUZINOV, S. MINKO and W. WILKE, in "ECCM CTS2 2nd European Conference on Composite Materials, Composite Testing and Standardisation", Hamburg edited by P. J. Hogg, K. Schulta and H. Wittich (Woodhead, Cambridge, 1994).
9. L. LORENZO and H. T. HAHN, *J. Acoust. Emission* **5** (1986) 15.
10. M. FAUDREE, E. BAER, A. HILTNER and J. COLLISTER, *J. Compos. Mater.* **22** (1988) 1170.
11. S. SHIROUZU, S. SHICHIJYO, S. TAKI, K. MATSUSHIGE, K. TAKAHASHI and T. TAKEMURA, *Polym. J.* **16** (1984) 223.
12. M. BRATRICH, B. HEISE, R. KRAUS, G. VOLSWINKLER, W. WILKE, G. BODOR and A. KALLÓ, *Müanyag és Gumi* **28** (1991) 273.
13. A. PAYER, Doctoral thesis, University of Ulm, in preparation (1997).

Received 23 February 1996
and accepted 10 February 1997